

University of Groningen

## The Primary Photochemistry of Vision Occurs at the Molecular Speed Limit

Johnson, Philip J. M.; Farag, Marwa H.; Halpin, Alexei; Morizumi, Takefumi; Prokhorenko, Valentyn I.; Knoester, Jasper; Jansen, Thomas L. C.; Ernst, Oliver P.; Miller, R. J. Dwayne

*Published in:*

The Journal of Physical Chemistry. B: Materials, Surfaces, Interfaces, & Biophysical

*DOI:*

[10.1021/acs.jpcc.7b02329](https://doi.org/10.1021/acs.jpcc.7b02329)

**IMPORTANT NOTE: You are advised to consult the publisher's version (publisher's PDF) if you wish to cite from it. Please check the document version below.**

*Document Version*

Publisher's PDF, also known as Version of record

*Publication date:*

2017

[Link to publication in University of Groningen/UMCG research database](#)

*Citation for published version (APA):*

Johnson, P. J. M., Farag, M. H., Halpin, A., Morizumi, T., Prokhorenko, V. I., Knoester, J., Jansen, T. L. C., Ernst, O. P., & Miller, R. J. D. (2017). The Primary Photochemistry of Vision Occurs at the Molecular Speed Limit. *The Journal of Physical Chemistry. B: Materials, Surfaces, Interfaces, & Biophysical*, 121(16), 4040-4047. <https://doi.org/10.1021/acs.jpcc.7b02329>

### Copyright

Other than for strictly personal use, it is not permitted to download or to forward/distribute the text or part of it without the consent of the author(s) and/or copyright holder(s), unless the work is under an open content license (like Creative Commons).

The publication may also be distributed here under the terms of Article 25fa of the Dutch Copyright Act, indicated by the "Taverne" license. More information can be found on the University of Groningen website: <https://www.rug.nl/library/open-access/self-archiving-pure/taverne-amendment>.

### Take-down policy

If you believe that this document breaches copyright please contact us providing details, and we will remove access to the work immediately and investigate your claim.

*Downloaded from the University of Groningen/UMCG research database (Pure): <http://www.rug.nl/research/portal>. For technical reasons the number of authors shown on this cover page is limited to 10 maximum.*

# The Primary Photochemistry of Vision Occurs at the Molecular Speed Limit

Philip J. M. Johnson,<sup>†</sup> Marwa H. Farag,<sup>‡,§</sup> Alexei Halpin,<sup>†</sup> Takefumi Morizumi,<sup>||</sup> Valentyn I. Prokhorenko,<sup>§</sup> Jasper Knoester,<sup>‡</sup> Thomas L. C. Jansen,<sup>‡</sup> Oliver P. Ernst,<sup>||,⊥</sup> and R. J. Dwayne Miller<sup>\*,†,§,Ⓜ</sup>

<sup>†</sup>Departments of Chemistry & Physics, University of Toronto, 80 St. George Street, Toronto, Ontario M5S 3H6, Canada

<sup>‡</sup>Zernike Institute for Advanced Materials, University of Groningen, Nijenborgh 4, 9747 AG Groningen, The Netherlands

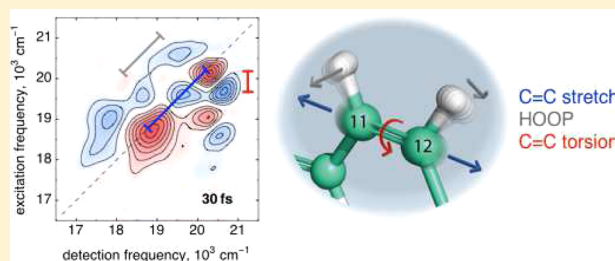
<sup>§</sup>Max Planck Institute for the Structure and Dynamics of Matter, Atomically Resolved Dynamics Division, Luruper Chaussee 149, Hamburg 22761, Germany

<sup>||</sup>Department of Biochemistry, University of Toronto, 1 King's College Circle, Toronto, Ontario M5S 1A8, Canada

<sup>⊥</sup>Department of Molecular Genetics, University of Toronto, 1 King's College Circle, Toronto, Ontario M5S 1A8, Canada

## Supporting Information

**ABSTRACT:** Ultrafast photochemical reactions are initiated by vibronic transitions from the reactant ground state to the excited potential energy surface, directly populating excited-state vibrational modes. The primary photochemical reaction of vision, the isomerization of retinal in the protein rhodopsin, is known to be a vibrationally coherent reaction, but the Franck–Condon factors responsible for initiating the process have been difficult to resolve with conventional time-resolved spectroscopies. Here we employ experimental and theoretical 2D photon echo spectroscopy to directly resolve for the first time the Franck–Condon factors that initiate isomerization on the excited potential energy surface and track the reaction dynamics. The spectral dynamics reveal vibrationally coherent isomerization occurring on the fastest possible time scale, that of a single period of the local torsional reaction coordinate. We successfully model this process as coherent wavepacket motion through a conical intersection on a  $\sim 30$  fs time scale, confirming the reaction coordinate as a local torsional coordinate with a frequency of  $\sim 570$   $\text{cm}^{-1}$ . As a result of spectral features being spread out along two frequency coordinates, we unambiguously assign reactant and product states following passage through the conical intersection, which reveal the key vibronic transitions that initiate the vibrationally coherent photochemistry of vision.



## INTRODUCTION

Dim light vision is facilitated by the rod photoreceptor rhodopsin, a seven transmembrane  $\alpha$ -helical protein with a covalently bound light-sensitive retinal chromophore, initially in an 11-*cis* configuration.<sup>1</sup> Absorption of a photon results in ultrafast isomerization of the retinal chromophore to an all-*trans* configuration, a process that was initially identified to occur within  $\sim 200$  fs<sup>2,3</sup> and is now attributed to a conical intersection between the excited- and ground-state potential energy surfaces,<sup>4,5</sup> which allows for efficient photointermediate formation. These features have made rhodopsin a canonical system for the study of nonadiabatic photochemistry, but despite considerable experimental<sup>6–9</sup> and theoretical<sup>4,5,10</sup> efforts, controversy remains surrounding the kinetics of isomerization and the effects of vibrational motion of the retinal chromophore on barrier crossing. The specific nature of the reaction coordinate for retinal isomerization in rhodopsin is thus still not fully understood.

As a result of the extremely short time scale for the isomerization reaction in rhodopsin, coherent nuclear motions were hypothesized to play a role in the reaction mechanism,

and long-lived low-frequency vibrational coherences identified as delocalized torsional motion of the retinal chromophore were observed to modulate the photoinduced absorption of the primary bathorhodopsin intermediate.<sup>11,12</sup> More recently, highly sensitive transient absorption measurements have revealed the full vibrational manifold of the reactant and primary photointermediate states of the retinal chromophore,<sup>6</sup> while transient grating measurements resolved a truly coherent photointermediate formation event on a  $\sim 50$  fs time scale.<sup>13</sup> All other transient spectroscopic measurements of retinal isomerization in rhodopsin reported on a slower  $\sim 200$  fs time scale for photoproduct formation, largely due to the significant overlap between reactant and photoproduct absorption bands. This led to the interpretation that the reaction coordinate was composed of a low-frequency delocalized torsional vibration. The most recent transient grating measurements, however, implicate the local  $C_{11}=C_{12}$  torsional mode as the reaction

Received: March 11, 2017

Revised: March 29, 2017

Published: March 30, 2017

coordinate, with coupling to local ethylenic stretching and out-of-plane hydrogen wagging acting in concert to drive the primary photochemistry of vision. However, significant spectral overlap between reactant, intermediate, and product states still limits a complete understanding of the coherent vibrational motion and passage through the conical intersection during isomerization.

The observation of such coherent vibrational motion from time-resolved spectroscopic studies strongly implies that vibronic transitions are the origin of the unique vibrationally coherent properties of retinal isomerization in vision. Resonance Raman scattering studies of rhodopsin<sup>14–16</sup> identified the  $\sim 1550\text{ cm}^{-1}$  in-phase ethylenic stretch mode as the dominant Raman-active high-frequency vibration, with secondary activity from the  $\sim 970\text{ cm}^{-1}$   $\text{HC}_{11}=\text{C}_{12}\text{H}$  out-of-plane wags, while significant displacements were also observed for low-frequency ( $<400\text{ cm}^{-1}$ ) delocalized torsional vibrations. A detailed Franck–Condon analysis of the linear absorption spectrum of rhodopsin based on these resonance Raman intensities attributed the extremely broad absorption band to a Franck–Condon progression of the in-phase ethylenic stretch, while the lack of clear vibronic features in the room-temperature spectrum was assigned to the low-frequency modes that act to spectrally broaden the high-frequency Franck–Condon progression.<sup>17</sup> Despite the effectively featureless and homogeneous linear absorption spectrum of rhodopsin (even, in fact, at  $4\text{ K}$ <sup>18</sup>), spectral evidence of the vibronic coupling arising from a Franck–Condon progression of the ethylenic stretch vibration was observed in the transient-grating response of bovine rhodopsin, persisting for the first  $\sim 100\text{ fs}$  after photoexcitation.<sup>13</sup>

To determine the effects of vibronic coupling on the vibrationally coherent photointermediate formation in rhodopsin, we present a combined experimental and theoretical study of the two-dimensional photon echo (2DPE) response of retinal isomerization in bovine rhodopsin. The additional pump frequency resolution of the 2DPE approach<sup>19–22</sup> to the spectral response of the retinal chromophore allows for a less congested view of photoisomerization and observation of the coupling between components of the linear absorption spectrum directly in the spectral domain as a function of waiting time. This allows us to directly observe the underlying Franck–Condon factors and the subsequent evolution of these vibronic couplings on the nonadiabatic dynamics of the isomerization reaction.

## METHODS SECTION

**Sample Preparation.** Rod outer segments (ROS) were isolated from frozen bovine retinae (WL Lawson Company, Omaha, NE) using standard discontinuous sucrose density gradient methods.<sup>23</sup> The ROS membranes were then treated with  $4\text{ M}$  urea in hypotonic buffer ( $10\text{ mM}$  Tris,  $1\text{ mM}$  EDTA,  $\text{pH } 8.0$ ) and were repeatedly washed with hypotonic buffer without urea ( $10\text{ mM}$  Tris,  $1\text{ mM}$  EDTA,  $\text{pH } 7.2$ ) to remove membrane-associated proteins.<sup>24</sup> The washed membranes were then solubilized by  $1.5\%$  *n*-dodecyl  $\beta$ -D-maltoside in isotonic buffer ( $20\text{ mM}$  Tris,  $100\text{ mM}$  NaCl,  $2\text{ mM}$   $\text{MgCl}_2$ ,  $\text{pH } 7.2$ ); then, the extracted rhodopsin was concentrated to  $10\text{ mg/mL}$  using a  $30\text{ kDa}$  MWCO centrifugal ultrafiltration device (Millipore). The concentrated sample was then aliquoted, flash-frozen, and stored at  $-80\text{ }^\circ\text{C}$ . The sample concentration was estimated from its absorbance at the absorption maximum (molar extinction coefficient at  $500\text{ nm} = 40\,600\text{ M}^{-1}\text{cm}^{-1}$ <sup>25</sup>). All procedures were performed at  $4\text{ }^\circ\text{C}$  and under dim red light.

**Experimental Photon Echo Spectroscopy.** Photon echo spectra<sup>26</sup> of the isomerization dynamics of retinal in rhodopsin were performed using  $11\text{ fs}$  pulses having an energy of  $10\text{ nJ/beam}$ . The local oscillator, used for heterodyne detection, was attenuated by OD 2, with a temporal delay of  $\sim 325\text{ fs}$  introduced by the optical path length of the OD filter itself. The coherence time  $t_1$  was scanned over the range  $[-50, 50]\text{ fs}$  in  $1.6\text{ fs}$  steps, and 50 spectra were averaged per  $t_1$  delay. Precise determination of the LO delay (and therefore phasing) was determined by comparison of the pump–probe response to the heterodyne echo about  $t_1 = t_2 = 0\text{ fs}$ , measured sequentially in the 2DPE spectrometer. 2D spectra were subsequently collected for population times between  $[0, 100]\text{ fs}$  in  $5\text{ fs}$  intervals and coarse-grained sampling of longer waiting times thereafter (see Figure 2 and SI). A  $150\text{ cm}^{-1}$  square moving average has been applied to the data.

**Computational Details.** Simulations of the 2DPE spectroscopy of rhodopsin were performed in the impulsive limit by employing a fully quantum-mechanical model.<sup>27,28</sup> The model consists of two diabatic electronic states and two nuclear degrees of freedom (the localized torsional mode, which defines the *cis*-to-*trans* isomerization, and a coupling mode, the in-phase ethylenic stretch, which couples the electronic states to first order). The other 26 Franck–Condon active vibrational modes of the retinal chromophore in rhodopsin<sup>16</sup> were added as a weakly coupled quantum bath. The total wave function was then defined as the product of the wave function of the system, which is treated numerically exactly, and the wave function of the bath, which is treated via the time-dependent Hartree approach. For further details, see the Supporting Information.

## RESULTS AND DISCUSSION

**Coherent Isomerization Dynamics.** 2DPE spectra were measured with resonant  $\sim 11\text{ fs}$  pulses<sup>29</sup> with sufficient spectral bandwidth to allow for the observation of vibronic effects up to and including the in-phase ethylenic stretch frequency as well as the appearance of photoinduced absorption resulting from the formation of the primary photointermediate with an all-*trans* retinal chromophore. 2DPE spectra were collected at waiting times between  $0$  and  $100\text{ fs}$  in  $5\text{ fs}$  steps and select waiting times thereafter (see the Supporting Information for the complete set of experimental spectra). Theoretical calculations of the multidimensional spectral response in the impulsive limit were performed with a two-state, two-mode model,<sup>27,28</sup> as depicted with adiabatic potential energy surfaces in Figure 1A. This minimal model consists of ground and excited electronic states along a torsional reaction coordinate defined by the local  $\text{C}_{11}=\text{C}_{12}$  double bond, with the in-phase ethylenic stretching mode as the coupling coordinate. The nuclear coordinates and coupling parameters of the two-state, two-mode model were modified from refs 24 and 25 to simultaneously reproduce both the linear absorption spectrum and the kinetics of the primary photointermediate state due to the ultrafast isomerization of retinal. Vertical transitions due to the Franck–Condon progression of the ethylenic stretch coupling coordinate (Figure 1B) lead to the extremely broad linear absorption of rhodopsin (Figure 1C). The vibrationally coherent isomerization dynamics that result from Franck–Condon states that directly populated excited-state vibrational modes should thus be readily observed by 2DPE spectroscopy.

The experimental 2DPE spectra of retinal isomerization in rhodopsin are shown in Figure 2 (top row) for select waiting times. At the earliest waiting time ( $t_2 = 15\text{ fs}$ ), we observe clear

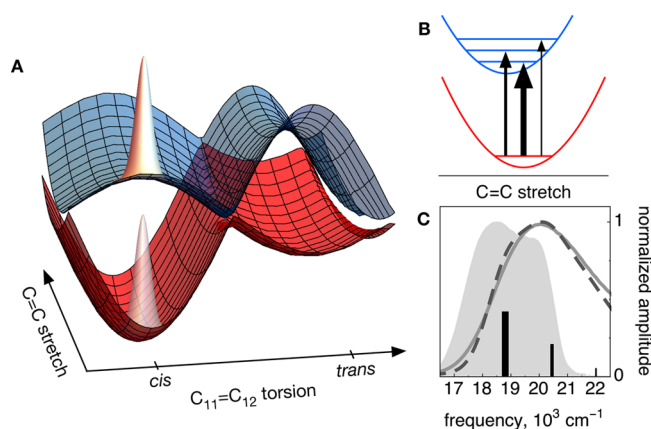


**Figure 1.** Minimal model of the potential energy surfaces of the isomerization of retinal in rhodopsin. (A) Adiabatic potential energy surfaces in a two-state, two-mode model consisting of an isomerization reaction coordinate, chosen to be the local  $C_{11}=C_{12}$  torsion, and the coupling coordinate, chosen to be the in-phase  $C=C$  stretch, which allows for vibronic coupling between the ground (red) and excited state (blue) surfaces. A wavepacket is shown at the Franck–Condon region following vertical excitation from the ground state. (B) Vibronic transitions from the ground state to the excited state of the coupling coordinate with vibrational quanta  $\nu = 0, 1,$  and  $2$  are shown with relative intensities (depicted by line thickness) obtained from previous resonance Raman studies. (C) Linear absorption spectrum of rhodopsin (experimental: solid gray line; simulated: dashed black line) with the corresponding Franck–Condon progression (absolute frequencies and approximate amplitudes taken from ref 13 are shown in solid black). The experimental laser spectrum is shown filled in light gray.

signatures of vibronic coupling<sup>30,31</sup> manifest as two distinct bleach bands (red contours), one along the diagonal at the linear absorption maximum of  $\sim 20\,000\text{ cm}^{-1}$  and a very prominent cross peak above the diagonal indicating coupling

between excitation of the linear absorption maximum and a bleach response detected at a red-shifted frequency of  $\sim 18\,500\text{ cm}^{-1}$ . These features are consistent with the Franck–Condon analysis of the transitions that comprise the linear absorption spectrum of rhodopsin, with a frequency splitting commensurate with the in-phase ethylenic stretch frequency.<sup>17</sup> Within a waiting time of 65 fs, we continue to observe off-diagonal bleach signals indicating coupling between the now-prominent on-diagonal bleach bands, and a red-shifted absorptive contribution (blue contours) at a detection frequency of  $\sim 18\,000\text{ cm}^{-1}$  appears prominently in the spectrum, which persists for all remaining waiting times shown. This feature is assigned to the formation of the primary photointermediate with an all-*trans* retinal chromophore as a result of passage from the excited state to the photointermediate ground-state surface through a conical intersection.<sup>13</sup> At longer waiting times we observe the onset of spectral diffusion of the bleach response, which leads to a significant loss of structure and a more homogeneous 2D spectrum, while only minor amplitude changes are observed in the photoinduced absorption band.

Calculations of the 2D spectra of the two-state, two-mode model show similar spectral features (Figure 2, bottom row), most prominently the splitting between bleach components due to ethylenic coupling at the same absolute frequencies as in the experimental data. In addition, cross peaks are observed both above and below the diagonal, where, as a result of the impulsive limit used for the calculations, the complete vibronic progression along both excitation and detection frequency axes is resolved. On a similar time scale, set by defining the reaction coordinate to be the local  $570\text{ cm}^{-1}$   $C_{11}=C_{12}$  torsion, the appearance of an absorptive band attributed to the isomerization of the retinal chromophore to an all-*trans* configuration is observed at a detection frequency of  $\sim 17\,500\text{ cm}^{-1}$ , as is unambiguously resolved in the experimental data. This is demonstrated in Figure 3, where the theoretical spectra presented in Figure 2 are

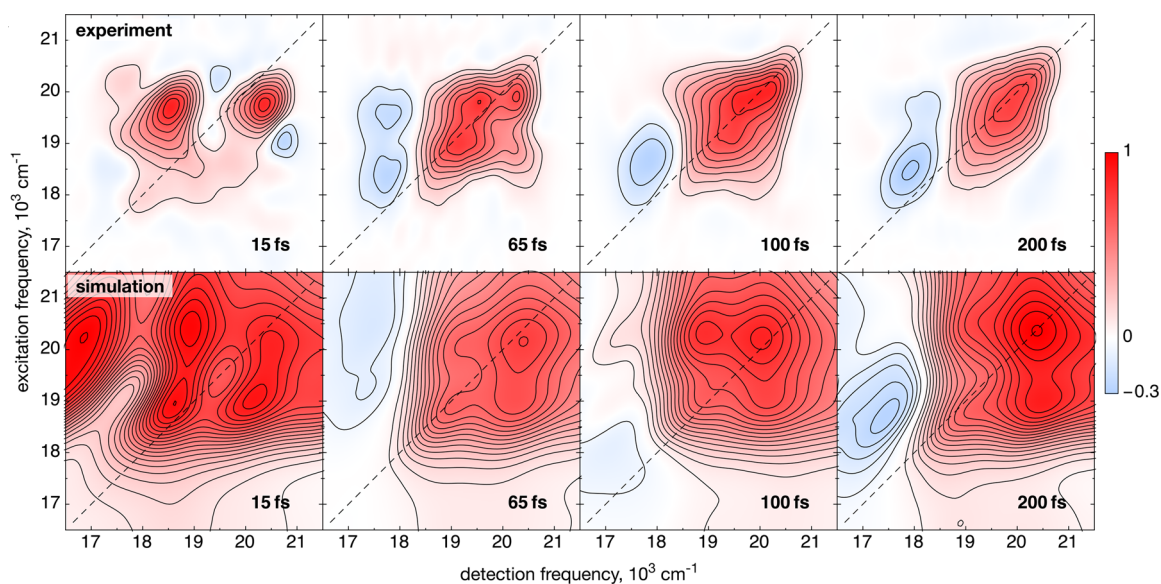


**Figure 2.** 2D photon echo spectroscopy of retinal isomerization in rhodopsin. Experimental 2DPE spectra with  $\sim 11$  fs resonant pulses (top row) and calculated 2DPE spectra in the impulsive limit (bottom row) at select waiting times reveal the vibronic coupling of the in-phase ethylenic stretch vibration to the photoinduced transition and the rapid appearance of a red-shifted photointermediate absorption band of the primary photointermediate photorhodopsin as a result of coherent torsional motion of the retinal chromophore about the local  $C_{11}=C_{12}$  isomerization reaction coordinate. Contours for experimental spectra are drawn in  $\pm 10\%$  intervals of the maximum experimental amplitude. Contours for the simulated spectra are drawn at  $\pm 5\%$  intervals of the maximum of the simulated spectral amplitudes.

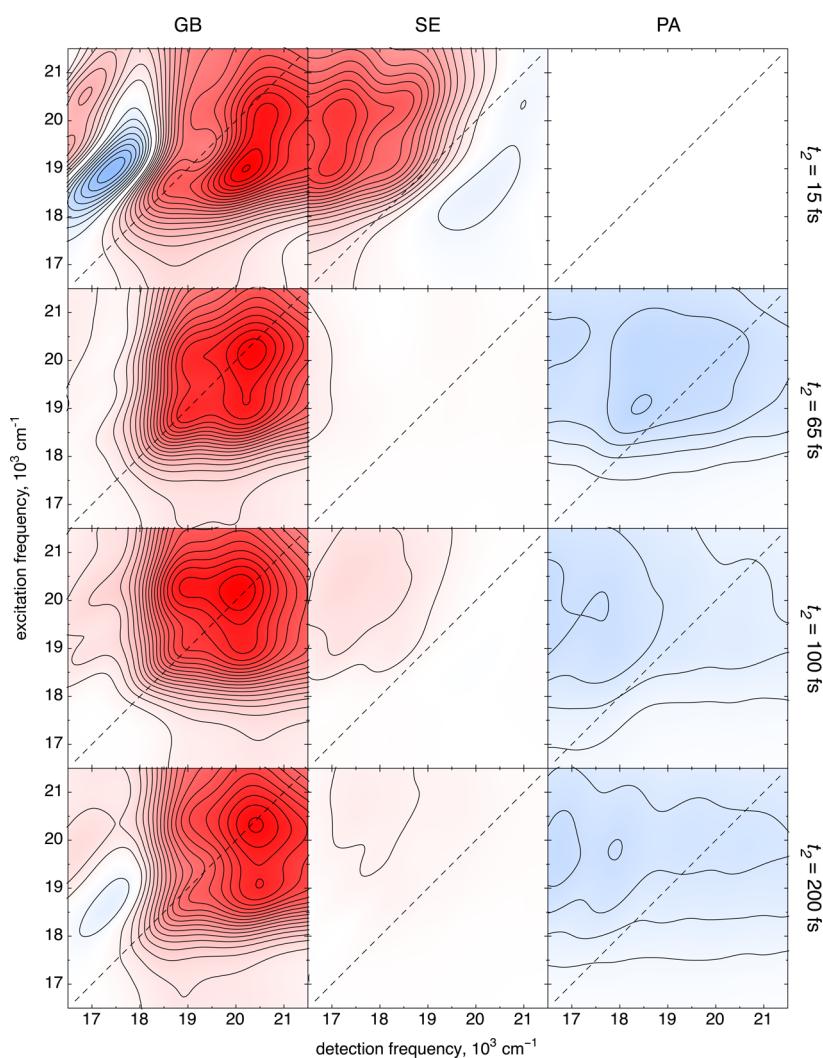


**Figure 3.** Contribution from the ground state bleach (GB), stimulated emission (SE), and photoinduced absorption (PA) to the total 2DPE spectra (see Figure 2).

separated in contributions from the ground-state bleach (GB), stimulated emission (SE), and photoinduced absorption (PA). The stimulated emission spectra have a negligible contribution after the wavepacket has passed through the conical intersection. Following passage through the conical intersection, a photoinduced absorption signal is generated as a result of the formation of the photoproduct. The decomposition in Figure 3 shows that the negative features (blue contours) found in the 2DPE at  $T = 65, 100, 200$  fs reflect the absorption of the *trans* photoproduct, while the positive features (red contours) correspond to the bleach of the reactant *cis* isomer ground-state absorption. This result confirms that the isomerization reaction of retinal in the protein rhodopsin occurs via concerted torsional motion about the local  $C_{11}=C_{12}$  double bond, passing through the conical intersection on a  $\sim 30$  fs time scale, in concurrence with the half-period of this vibration. Whereas previous calculations with a similar model employed a lower frequency ( $\sim 240$   $\text{cm}^{-1}$ ) delocalized mode as the reaction coordinate,<sup>27,28</sup> such parameters dramatically overestimate the arrival time of the all-*trans* photointermediate (see Supporting Information), and we thus conclude that the isomerization of retinal in rhodopsin represents a truly coherent surface crossing event on the time scale of a single period of the local torsional motion.

**Cross-Peak Dynamics.** The temporal evolution of cross peaks in multidimensional spectra has commanded significant interest and has been used as a marker to assign ground- versus excited-state origin to spectral dynamics.<sup>32,33</sup> The cross peaks associated with the ethylenic stretch splitting (see Figure 4) persist beyond the first 100 fs following photoexcitation, which are monitored by spectral integration of the square regions highlighted in Figure 4A at conjugate corners of the 2D spectrum. Following the surface crossing event, we observe (see Figure 4B) nearly perfectly anticorrelated oscillations (relative phase difference of  $\sim \pi/1.85$ ) with a periodicity commensurate with the frequency splitting between the on-diagonal bleach features ( $\sim 21$  fs) and dephasing times in excess of the temporal window of the measurement ( $>200$  fs). Such anticorrelation between conjugate cross peaks has previously been assigned to out-of-phase wave-packet motion simultaneously on both the excited- and ground-state potentials<sup>32,33</sup> in the context of a displaced harmonic oscillator model, and it might be reasonable to assume the relevance of this model to the in-phase C=C stretch mode, as depicted by the potentials in Figure 1. However, the excited-state lifetime for rhodopsin is extremely short,<sup>13</sup> and we would thus expect significantly faster damping for an excited-state wave packet than is experimentally observed.

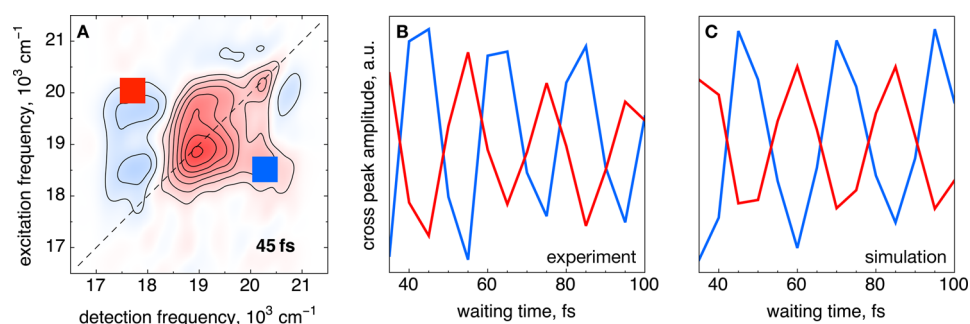


**Figure 4.** Vibronic cross-peak dynamics. (A) 2D photon echo response at a waiting time of  $t_2 = 45$  fs, with red and blue boxes above and below the diagonal, respectively, indicating spectral regions for analysis of cross-peak dynamics. (B) Experimental cross-peak dynamics following barrier crossing, where we observe a near perfectly anticorrelated cross-peak amplitude above and below the diagonal with a period commensurate with the in-phase ethylenic stretch frequency. (C) Simulations allow for isolation of the specific spectral contribution to total four-wave mixing signal, which reveals that coherent wave packet motion along the ground-state surface is the source of the anticorrelated cross-peak oscillation.

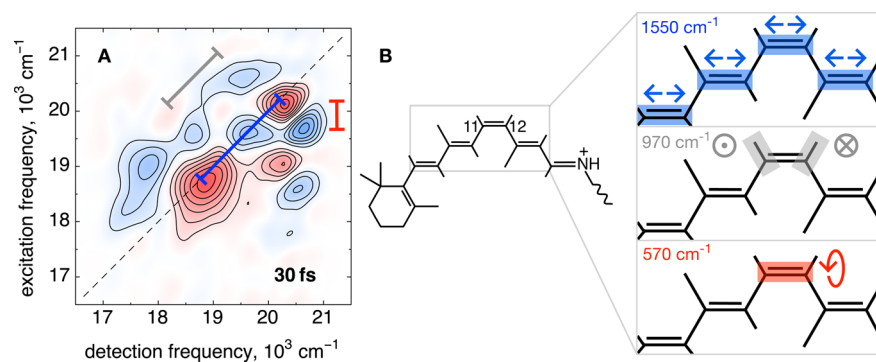


**Figure 5.** Photon echoes of the vibrational origin of vision. (A) 2D photon echo response at a waiting time  $t_2 = 30$  fs, which is the half-period of the local torsional isomerization coordinate. As a result of excited-state wave packet leaving the resonant spectral window, the Franck–Condon states responsible for the coherent nuclear response of retinal in rhodopsin are revealed. Three dominant frequency splittings from the linear absorption maximum are observed, consisting of the  $\sim 1550$   $\text{cm}^{-1}$  in phase-delocalized ethylenic stretch vibration (indicated by the blue line along the diagonal), the  $\sim 970$   $\text{cm}^{-1}$  ground-state hydrogen out-of-plane oscillation from the  $\text{C}_{11}$  and  $\text{C}_{12}$  hydrogens (indicated by the gray line above the diagonal), and the  $\sim 570$   $\text{cm}^{-1}$   $\text{C}_{11}=\text{C}_{12}$  torsional mode (indicated by the vertical red line). (B) Schematic of the 11-*cis* retinal chromophore of rhodopsin and the above vibrational normal modes recovered from 2DPE spectroscopy which lead to the ultrafast and vibrationally coherent primary photochemistry of rhodopsin.

The resolution of this discrepancy is found through analysis of the pathways that make up the calculated 2DPE spectra. Contributions from the rephasing and nonrephasing response from the ground-state bleach, stimulated emission, and photo-intermediate absorption can be isolated computationally (see Figure 3), and analysis of the calculated contributions allows for the unequivocal assignment of the anticorrelated oscillation between the above and below diagonal cross peaks to the rephasing component of the ground-state bleach response, which is shown in Figure 4C. A slight discrepancy in periodicity is observed between the calculated ( $\sim 24$  fs) and experimental ( $\sim 21$  fs) response and can be attributed to details of both the experiment and the calculations. Experimentally, a great many high-frequency modes can contribute in this frequency region,<sup>13</sup> and it is not possible to isolate the response due solely to the cross peak itself, even with narrow spectral integration. On the computational side, anharmonicity is introduced along the  $\text{C}=\text{C}$  stretch coordinate by the coupling between surfaces, as depicted in Figure 1, which acts to slightly decrease (increase) the frequency (period) of oscillation on the ground state while slightly increasing (decreasing) the frequency (period) of the  $\text{C}=\text{C}$  stretch oscillation on the excited state.<sup>34</sup> Such a clear assignment of anticorrelated cross-peak dynamics to a strictly ground-state process indicates the great care that must be taken when interpreting 2D spectral dynamics.

**Franck–Condon States.** While the in-phase  $\text{C}=\text{C}$  stretch contribution to the spectral dynamics following photoexcitation is clear, vibronic transitions from other high-frequency modes<sup>35</sup> would also be expected, particularly the ground-state hydrogen wagging vibration about the  $\text{HC}_{11}=\text{C}_{12}\text{H}$  coordinate with a frequency of  $\sim 970$   $\text{cm}^{-1}$  and, based on recent transient-grating experiments,<sup>13</sup> the ground-state local  $\text{C}_{11}=\text{C}_{12}$  torsion with a frequency of  $\sim 570$   $\text{cm}^{-1}$ . From the Franck–Condon analysis of the linear absorption spectrum it is predicted that the absorption maximum of rhodopsin is composed of three transitions about  $\nu = 20\,000$   $\text{cm}^{-1}$  arising from vibronic coupling to modes with frequencies in excess of  $500$   $\text{cm}^{-1}$ .<sup>17</sup> The early response of rhodopsin (e.g., the  $t_2 = 15$  fs spectra of Figure 2) is dominated by the vibronic response of the ethylenic stretch but does not show any significant additional structure. However, as the excited-state wave packet leaves the resonant Franck–Condon region<sup>12</sup> contributions from the stimulated emission pathways diminish and we would expect them to be minimal at a waiting time commensurate with surface crossing through the conical intersection between the excited- and ground-state surfaces, where the  $\text{C}_{11}=\text{C}_{12}$  dihedral angle would be rotated by  $\pi/2$  from the *cis* configuration. For the vibrationally coherent isomerization in rhodopsin, this occurs at a waiting time of  $t_2 = 30$  fs,<sup>13</sup> and the residual resonant spectral signatures reveal the vibronic origin of vision.

The experimental 2D spectrum at the waiting time associated with the transition through the conical intersection is shown in Figure 5A, and a number of dramatic features are readily observed. Vibronic coupling has been shown to result in a grid-like distribution of on- and off-diagonal peaks, reporting on the intramolecular vibrations that couple to the optical transition.<sup>31,36</sup> As a result of incomplete vibronic dephasing, we observe these features in both the ground-state bleach response as well as in the nascent absorptive signals due to the photoisomerization state as well. In contrast with the expectation that spectral diffusion would act to monotonically decrease structure in the 2D spectrum as a function of waiting time we observe the bleach response to narrow considerably, becoming sharply defined peaks along the diagonal. The absorptive transitions display similarly narrow lineshapes in the 2D spectrum, with characteristic frequency splittings between peaks associated with the ground-state frequencies described above, shown schematically in Figure 5B. First, the in-phase ethylenic stretch vibration figures prominently along the diagonal at this waiting time, as indicated by the blue line. Second, the gray line above the diagonal indicates peaks with  $\sim 970\text{ cm}^{-1}$  frequency splitting consistent with the ground-state HOOP wag. Finally, the vertical red line highlights an off-diagonal peak with a frequency splitting of  $\sim 570\text{ cm}^{-1}$  from the linear absorption maximum, corresponding to the local torsional mode of the isomerization coordinate itself.

The two-state, two-mode model accounts for the vast majority of experimental observations. However, the grid-like distribution of interfering peaks, reporting from the strongly coupled intramolecular vibrations as observed on intermediate waiting times, is not reproduced by theory. Accounting for these details would require a substantially more complicated model, incorporating additional vibrational modes as well as the higher-lying excited potential surfaces giving rise to the observed absorptive features. The number of free parameters necessary for such a model calls for high accuracy *ab initio* calculations of the potential energy surfaces.<sup>37</sup> A more detailed account of bath correlation times and the inclusion of finite pulse effects<sup>38</sup> may further improve the comparison between theory and experiment for intermediate waiting times. The combination of homogeneous and inhomogeneous broadening needed to model the present 2D spectra, as described in the SI, further clearly demonstrates that 2D spectra provide extra constraints for theory. As such, the spectral dynamics presented here provide unique information to guide future calculations of the primary photochemistry of vision and other ultrafast photochemical dynamics initiated by vertical transitions due to Franck–Condon factors.

## CONCLUSIONS

The picture that emerges of the primary photochemistry of vision is that of a breakdown in the Born–Oppenheimer approximation leading to coupling between vibrational and electronic degrees of freedom. Resonance Raman scattering of rhodopsin has long shown the extent of vibrational coupling to the electronic transition, where the extremely broad and featureless linear absorption spectrum is a result of the Franck–Condon progression of the highly displaced in-phase ethylenic stretch vibration with coupling to low-frequency torsional modes and to the surrounding protein environment (the bath). Subsequent time-resolved spectroscopies revealed the evolution of these crucial nuclear motions during the

photochemical reaction through the existence of long-lived vibrational coherences persisting to the ground-state of the photointermediate absorption band. More recent measurements identified strictly local stretches, out-of-plane wags, and torsional activity about the  $C_{11}=C_{12}$  isomerization coordinate as the modes that couple to and drive the isomerization reaction. Now, experimental and theoretical multidimensional photon echoes have brought the observations full circle. Experimental 2D spectroscopy unambiguously resolved a photoproduct formation event on a  $\sim 60\text{ fs}$  time scale, and simulations employing a model of the reaction coordinate assigned to the local  $C_{11}=C_{12}$  torsional mode confirmed the vibrationally coherent nature of the isomerization reaction. The dominant Franck–Condon factors associated with the in-phase ethylenic stretch mode result in vibronic transitions that directly populate the excited state and are manifested in the 2DPE spectra as a vibronic progression along the diagonal and associated off-diagonal cross peaks, and we assign the observed anticorrelated cross-peak dynamics to a strictly ground-state response through analysis of the specific pathways that make up the simulated 2DPE spectra. Additional evidence of Franck–Condon states associated with both hydrogen out-of-plane wags and the  $C_{11}=C_{12}$  torsional mode were also observed in the experimental spectra. These transitions directly populate the excited-state vibrations necessary to drive the ultrafast primary photochemistry of vision (see Figure 6) within a single period ( $\sim 60\text{ fs}$ ) of the local  $C_{11}=C_{12}$  torsion, which represents a fundamental temporal limit for isomerization.

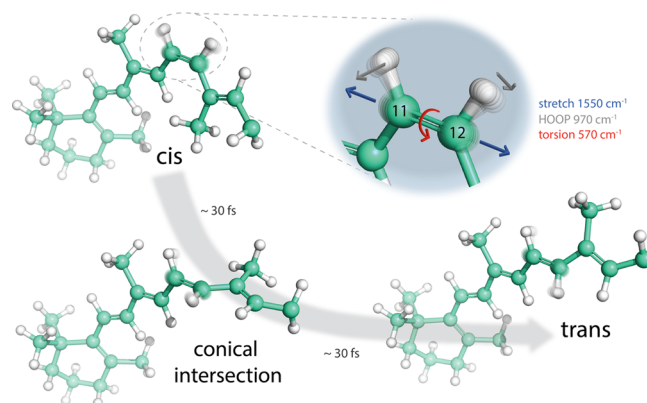


**Figure 6.** Isomerization of retinal in vision. Initially in an 11-*cis* configuration, photoexcitation of the retinal chromophore in rhodopsin results in vibronic transitions to the excited state, directly populating excited state vibrations of the key C=C stretch, torsion, and hydrogen out-of-plane wagging modes. The isomerization then proceeds along the C=C torsional coordinate, reaching the conical intersection in  $\sim 30\text{ fs}$ , where the torsional bond is rotated by  $\sim 90^\circ$ . Passing through the conical intersection with an efficiency of  $\sim 65\%$ , the *trans* configuration of the local torsional coordinate is reached within another  $\sim 30\text{ fs}$ , as observed by experimental and simulated photon echo spectroscopy in Figure 2.

## ASSOCIATED CONTENT

### Supporting Information

The Supporting Information is available free of charge on the ACS Publications website at DOI: 10.1021/acs.jpcc.7b02329.

Details regarding the simulated 2D spectra as well as a complete reproduction of all experimental 2D spectra. (PDF)

## AUTHOR INFORMATION

## Corresponding Author

\*E-mail: dwayne.miller@mpsd.mpg.de.

## ORCID

R. J. Dwayne Miller: 0000-0003-0884-0541

## Notes

The authors declare no competing financial interest.

## ACKNOWLEDGMENTS

We thank Maria Grigera and Lu Chen for excellent graphical and technical assistance, respectively. This research was supported by the Natural Sciences and Engineering Research Council of Canada (R.J.D.M.), the Max Planck Society (R.J.D.M.), the Canadian Institute for Advanced Research (R.J.D.M. and O.P.E.), and the Canada Excellence Research Chairs program (O.P.E.). O.P.E. is the Anne & Max Tanenbaum Chair in Neuroscience at the University of Toronto.

## REFERENCES

- (1) Ernst, O. P.; Lodowski, D. T.; Elstner, M.; Hegemann, P.; Brown, L. S.; Kandori, H. Microbial and Animal Rhodopsins: Structures, Functions, and Molecular Mechanisms. *Chem. Rev.* **2014**, *114*, 126–163.
- (2) Schoenlein, R. W.; Peteanu, L. A.; Mathies, R. A.; Shank, C. V. The First Step in Vision: Femtosecond Isomerization of Rhodopsin. *Science* **1991**, *254*, 412–415.
- (3) Peteanu, L. A.; Schoenlein, R. W.; Wang, Q.; Mathies, R. A.; Shank, C. V. The First Step in Vision Occurs in Femtoseconds: Complete Blue and Red Spectral Studies. *Proc. Natl. Acad. Sci. U. S. A.* **1993**, *90*, 11762–11766.
- (4) Frutos, L. M.; Andruniów, T.; Santoro, F.; Ferré, N.; Olivucci, M. Tracking the Excited-State Time Evolution of the Visual Pigment with Multiconfigurational Quantum Chemistry. *Proc. Natl. Acad. Sci. U. S. A.* **2007**, *104*, 7764–7769.
- (5) Schapiro, L.; Ryazantsev, M. N.; Frutos, L. M.; Ferré, N.; Lindh, R.; Olivucci, M. The Ultrafast Photoisomerizations of Rhodopsin and Bathorhodopsin are Modulated by Bond Length Alternation and HOOP Driven Electronic Effects. *J. Am. Chem. Soc.* **2011**, *133*, 3354–3364.
- (6) Schnedermann, C.; Liebel, M.; Kukura, P. Mode-Specificity of Vibrationally Coherent Internal Conversion in Rhodopsin during the Primary Visual Event. *J. Am. Chem. Soc.* **2015**, *137*, 2886–2891.
- (7) Bovee-Geurts, P. H. M.; Fernández, I. F.; Liu, R. S. H.; Mathies, R. A.; Lugtenburg, J.; DeGrip, W. J. Fluoro Derivative of Retinal Illuminates the Decisive Role of the C<sub>12</sub>-H Element in Photoisomerization and Rhodopsin Activation. *J. Am. Chem. Soc.* **2009**, *131*, 17933–17942.
- (8) Kukura, P.; McCamant, D. W.; Yoon, S.; Wandschneider, D. B.; Mathies, R. A. Structural Observation of the Primary Isomerization in Vision with Femtosecond-Stimulated Raman. *Science* **2005**, *310*, 1006–1009.
- (9) Wand, A.; Gdor, I.; Zhu, J.; Sheves, M.; Ruhman, S. Shedding New Light on Retinal Protein Photochemistry. *Annu. Rev. Phys. Chem.* **2013**, *64*, 437–458.
- (10) Weingart, O.; Altoè, Stenta, M.; Bottoni, A.; Orlandi, G.; Garavelli, M. Product Formation in Rhodopsin by Fast Hydrogen Motions. *Phys. Chem. Chem. Phys.* **2011**, *13*, 3645–3648.
- (11) Wang, Q.; Schoenlein, R. W.; Peteanu, L. A.; Mathies, R. A.; Shank, C. V. Vibrationally Coherent Photochemistry in the Femtosecond Primary Event of Vision. *Science* **1994**, *266*, 422–424.
- (12) Polli, D.; Altoè, P.; Weingart, O.; Spillane, K. M.; Manzoni, C.; Brida, D.; Tomasello, G.; Orlandi, G.; Kukura, P.; Mathies, R. A.; et al. Conical Intersection Dynamics of the Primary Photoisomerization Event in Vision. *Nature* **2010**, *467*, 440–443.
- (13) Johnson, P. J. M.; Halpin, A.; Morizumi, T.; Prokhorenko, V. I.; Ernst, O. P.; Miller, R. J. D. Local Vibrational Coherences Drive the Primary Photochemistry of Vision. *Nat. Chem.* **2015**, *7*, 980–986.
- (14) Eyring, G.; Curry, B.; Broek, A.; Lugtenburg, J.; Mathies, R. A. Assignment and Interpretation of Hydrogen Out-Of-Plane Vibrations in the Resonance Raman Spectra of Rhodopsin and Bathorhodopsin. *Biochemistry* **1982**, *21*, 384–393.
- (15) Palings, I.; Pardo, J. A.; van den Berg, E.; Winkel, C.; Lugtenburg, J.; Mathies, R. A. Assignment of Fingerprint Vibrations in the Resonance Raman Spectra of Rhodopsin, Isorhodopsin, and Bathorhodopsin: Implications for Chromophore Structure and Environment. *Biochemistry* **1987**, *26*, 2544–2556.
- (16) Lin, S. W.; Groesbeek, M.; van der Hoef, I.; Verdegem, P.; Lugtenburg, J.; Mathies, R. A. Vibrational Assignment of Torsional Normal Modes of Rhodopsin: Probing Excited-State Isomerization Dynamics along the Reactive C<sub>11</sub>=C<sub>12</sub> Torsion Coordinate. *J. Phys. Chem. B* **1998**, *102*, 2787–2806.
- (17) Loppnow, G. R.; Mathies, R. A. Excited-State Structure and Isomerization Dynamics of the Retinal Chromophore in Rhodopsin from Resonance Raman Intensities. *Biophys. J.* **1988**, *54*, 35–43.
- (18) Loppnow, G. R.; Mathies, R. A.; Middendorf, T. R.; Gottfried, D. S.; Boxer, S. G. Photochemical Hole-Burning Spectroscopy of Bovine Rhodopsin and Bacteriorhodopsin. *J. Phys. Chem.* **1992**, *96*, 737–745.
- (19) Hybl, J. D.; Albrecht, A.; Gallagher Faeder, S. M.; Jonas, D. M. Two-Dimensional Electronic Spectroscopy. *Chem. Phys. Lett.* **1998**, *297*, 307–313.
- (20) Cowan, M. L.; Ogilvie, J. P.; Miller, R. J. D. Two-Dimensional Spectroscopy Using Diffractive Optics Based Phased-Locked Photon Echoes. *Chem. Phys. Lett.* **2004**, *386*, 184–189.
- (21) Prokhorenko, V. I.; Halpin, A.; Miller, R. J. D. Coherently-Controlled Two-Dimensional Photon Echo Electronic Spectroscopy. *Opt. Express* **2009**, *17*, 9764–9779.
- (22) Ruetzel, S.; Diekmann, M.; Nuernberger, P.; Walter, C.; Engels, B.; Brixner, T. Multidimensional Spectroscopy of Photoreactivity. *Proc. Natl. Acad. Sci. U. S. A.* **2014**, *111*, 4764–4769.
- (23) Papermaster, D. S.; Dreyer, W. J. Rhodopsin Content in the Outer Segment Membranes of Bovine and Frog Retinal Rods. *Biochemistry* **1974**, *13*, 2438–2444.
- (24) Morizumi, T.; Imai, H.; Shichida, Y. Direct Observation of the Complex Formation of GDP-Bound Transducin with the Rhodopsin Intermediate having a Visible Absorption Maximum in Rod Outer Segment Membranes. *Biochemistry* **2005**, *44*, 9936–9943.
- (25) Wald, G.; Brown, P. K. The Molar Extinction of Rhodopsin. *J. Gen. Physiol.* **1953**, *37*, 189–200.
- (26) Prokhorenko, V. I.; Halpin, A.; Miller, R. J. D. Coherently-Controlled Two-Dimensional Photon Echo Electronic Spectroscopy. *Opt. Express* **2009**, *17*, 9764–9779.
- (27) Hahn, S.; Stock, G. Quantum-Mechanical Modeling of the Femtosecond Isomerization in Rhodopsin. *J. Phys. Chem. B* **2000**, *104*, 1146–1149.
- (28) Hahn, S.; Stock, G. Femtosecond Secondary Emission Arising from the Nonadiabatic Photoisomerization in Rhodopsin. *Chem. Phys.* **2000**, *259*, 297–312.
- (29) Johnson, P. J. M.; Prokhorenko, V. I.; Miller, R. J. D. Enhanced Bandwidth Noncollinear Optical Parametric Amplification with a Narrowband Anamorphic Pump. *Opt. Lett.* **2011**, *36*, 2170–2172.
- (30) Elsaesser, T.; Kaiser, W. Vibrational and Vibronic Relaxation of Large Polyatomic-Molecules in Liquids. *Annu. Rev. Phys. Chem.* **1991**, *42*, 83–107.
- (31) Krčmář, J.; Gelin, M. F.; Egorova, D.; Domcke, W. Signatures of Conical Intersections in Two-Dimensional Electronic Spectra. *J. Phys. B: At, Mol. Opt. Phys.* **2014**, *47*, 124019.
- (32) Caram, J. R.; Fidler, A. F.; Engel, G. S. Excited and Ground State Vibrational Dynamics Revealed by Two-Dimensional Electronic Spectroscopy. *J. Chem. Phys.* **2012**, *137*, 024507.
- (33) Bizimana, L. A.; Brazard, J.; Carbery, W. P.; Gellen, T.; Turner, D. B. Resolving Molecular Vibronic Structure Using High Sensitivity



Two-Dimensional Electronic Spectroscopy. *J. Chem. Phys.* **2015**, *143*, 164203.

(34) Farag, M. H.; Jansen, T. L. C.; Knoester, J. Probing the Interstate Coupling near a Conical Intersection by Optical Spectroscopy. *J. Phys. Chem. Lett.* **2016**, *7*, 3328–3334.

(35) While many low-frequency modes also display considerable amplitude in resonance Raman scattering, they act to broaden the spectral response and are thus not expected to appear as distinct peaks in the 2D spectra.

(36) Turner, D. B.; Dinshaw, R.; Lee, K.-K.; Belsley, M. S.; Wilk, K. E.; Curmi, P. M. G.; Scholes, G. D. Quantitative Investigations of Quantum Coherence for a Light-Harvesting Protein at Conditions Simulating Photosynthesis. *Phys. Chem. Chem. Phys.* **2012**, *14*, 4857–4874.

(37) Rivalta, I.; Nenov, A.; Weingart, O.; Cerullo, G.; Garavelli, M.; Mukamel, S. Modelling Time-Resolved Two-Dimensional Electronic Spectroscopy of the Primary Photoisomerization Event in Rhodopsin. *J. Phys. Chem. B* **2014**, *118*, 8396–8405.

(38) Tempelaar, R.; Halpin, A.; Johnson, P. J. M.; Cai, K.; Murphy, R. S.; Knoester, J.; Miller, R. J. D.; Jansen, T. L. C. Laser-Limited Signatures of Quantum Coherence. *J. Phys. Chem. A* **2016**, *120*, 3042–3048.